Response to Reviewers for "Optimally controlled NMR in electrochemistry: Larmor and nutation frequency selective spin excitation for locally selective NMR experiments"

Johannes F. Kochs[1,2,*], Armin J. Römer[1,2,*], Michael Schatz[1], Matthias Streun[3], Sven Jovanovic[1], Rüdiger-A. Eichel[1,4,5], Simone S. Köcher[1,6], and Josef Granwehr[1,2]

[1]Forschungszentrum Jülich GmbH, Institute of Energy Technologies, Fundamental Electrochemistry (IET-1), Jülich, Germany
[2]Institute of Technical and Macromolecular Chemistry, RWTH Aachen University, Aachen, Germany
[3]Forschungszentrum Jülich GmbH, Institute of Technology and Engineering (ITE), Jülich, Germany
[4]Institute of Physical Chemistry, RWTH Aachen University, Aachen, Germany
[5]Faculty of Mechanical Engineering, RWTH Aachen University, Aachen, Germany
[6]Fritz Haber Institute of the Max Planck Society, Berlin, Germany

Correspondence: Simone S. Köcher (s.koecher@fz-juelich.de)

Note for the Editor

We thank the Editor for considering our manuscript for publication in the journal *Magnetic Resonance Copernicus*, and the reviewers for their valuable comments that they have provided us with. In the current revision, we have addressed the comments made by the reviewers.

We were especially pleased that the reviewers appreciated our writing and presentation of the work, and that they recommended it for publication after revisions. Therefore, we believe that the revised version of the manuscript meets the criteria for publication in the journal *Magnetic Resonance Copernicus*.

We report below a detailed point-by-point answer to the reviewers' comments. As a convention, text in *italic black* is original text written by the reviewers. The text quoted from the article is:

- normal text if unchanged compared to the original version,
- green if added in the revised version,
- ~~strikethrough red if deleted (no longer in the revised article)~~.

We also attach a LatexDiff version, titled 'main-diff.pdf' of the manuscript with modifications with respect to the previous version marked.

1 Reviewer 2

In this article, the authors propose use of specially prepared RF pulses to selectively excite signals from two model liquids (water and n-dodecane) placed in a specially designed phantom made of plastic PEEK and copper disks. According to the authors, this phantom simulates an electrochemical cell for potentially conducting NMR measurements during electrochemical reactions directly within the NMR sprobe. Indeed, such experiments, for example, electrolysis or charging of chemical energy storage devices, are very interesting from an NMR perspective. However, as presented in the introduction, such measurements in complex heterogeneous structures using conductive metals, as well as other materials with magnetic susceptibilities different from those of the solvents, dramatically disrupt the homogeneity of the magnetic fields B0 and B1. Research aimed at finding solutions to these problems is extremely relevant.

The authors propose using the finite element method in conjunction with quantum optimal control to calculate specially prepared RF pulses for a specific phantom geometry or future electrochemical cell. This allows for selective signal excitation, for example, near electrodes or within the cell volume.

As a result of their work, the authors demonstrated the feasibility of their approach, specifically, they demonstrated that special pulses can selectively excite water protons in a PEEK cell and dodecane protons in a copper cell. They also demonstrated that signals from these liquids can be not only excited but also selectively suppressed in such a heterogeneous phantom. Convincing spectra and numerical parameters of the selectivity of these pulses are presented.

This work appears to be based on careful research and relates to the highly specialized field of NMR resonance. It demonstrates proof-of-concept of this approach rather than a ready-made algorithm for general use. Obviously, the pulses shown on Figures in the ESI will only work for the phantom presented in the article. I believe the work is worth publishing in the journal Magnetic Resonance Copernicus after minor revisions.

Response: We thank the reviewer for their thorough summary of our work and their detailed, productive comments.

The reviewer is correct, that this work presents a proof-of-concept for a rather specific FEM-QOC application for a particular, well defined phantom setup. However, the methodology and workflow can be readily adopted to different cell geometries, solvents, field strengths, and applications.

1. Figure 1 shows a diagram and a 3D view of the phantom. It needs to be improved. Why did you choose a huge font for the dimensions? Please make the font appropriate. The overall design isn't immediately clear; I think it would be helpful to show a three-dimensional cutout in the 3D view, like a slice of a pie, so the cell structure is clear. I would highlight the different liquids by different colors and label them in this Figure. Also, it would be helpful to show the location of the RF coil to scale compared to the phantom.

Response:

Thanks for the feedback on Fig. 1. Due to the cylindrical symmetry of the phantom, we do not see any benefit in three-dimensional cutout presentation suggested. We agree, that Fig. 1 is badly proportioned in particular with respect to the size of the labels. Instead of the RF coil, we depicted the homogenously NMR-sensitive volume which is centered between the lower copper and upper PEEK coin of the model setup and extends ± 4 mm in z-direction along the added z-axis.

Action:

We revised the figure in question.

Revised Paragraph:

Experimental Methods and Simulations

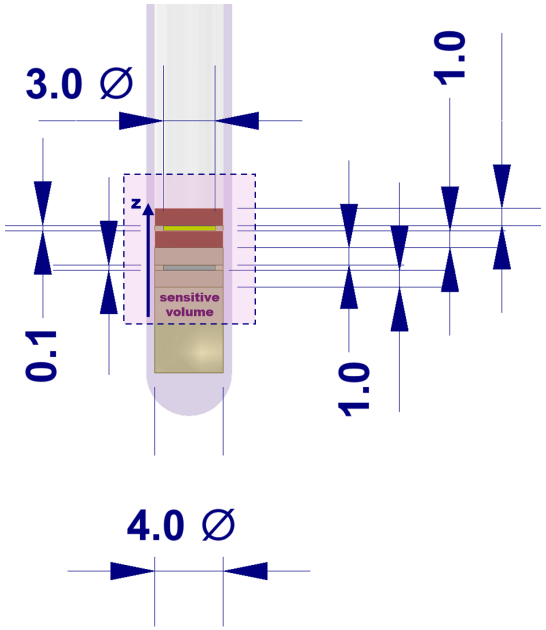

Figure 1: Sectional side view of experimental setup inside a shortened standard 5 mm NMR tube with cell dimensions given in mm (a) and 3D illustration of setup with a spatially-encoded chemical shift imaging of H_2O and *n*-dodecane in between the double coins (b). The cavities each have a diameter of 3 mm and a height of 0.1 mm. The coins each have a diameter of 4 mm and a height of 1 mm. The NMR-sensitive volume for homogeneous excitation is marked by a pink hue and extends ± 4 mm in z-direction from the center of the model setup. The spatial position of the liquids can be differentiated on a scale of about half a mm.

2. How were the liquids added to the cells? Were there any problems with air gaps? Could air gaps or bubbles also pose problems with B0 inhomogeneity?

Response:

The individual cavities were assembled separately. The components were immersed and assembled in the respective liquids, i.e. copper coins and PEEK separator in *n*-dodecane and PEEK coins and PEEK separator in H_2O. The sandwiched coins filled and coated with the respective solvent were removed from the liquid reservoir and combined within the NMR tube. Due to the surface tension of the liquids to the respective material, the coins adhered to the liquid and thus to another. Also, due to the small volume of the sandwiched liquid, any bubble or air gap would be very small on an absolute scale (max. 100 μm diameter), but simultaneously also counteract the adhesion between the coins, thus making them immediately noticeable in the cell construction. In conclusion, the formation of air gaps or bubbles cannot be rigorously eliminated, but their presence in the setup is highly unlikely.

Nonetheless, we would like to highlight that air bubbles potentially impact the B_0 homogeneity as has been demonstrated by Schatz et al. (2024) for air bubbles trapped underneath copper. We attempted to test the impact of air bubbles on a setup just consisting of PEEK coins and water. However, the susceptibility gradients across the microscopic liquid filled volume surrounded by polymer dominated the linewidth of the water signal (15 Hz full width at half maximum, 400-600 Hz of peak base width for a sample without air gaps), making the assessment of the air bubble impact on B_0 homogeneity difficult.

3. Line 152 describes the nutation experiments. It's not entirely clear what RF pulses were used for the nutation experiments. Specially optimized ones or simple hard rectangular ones. This should be specified.

Response:

Thank you for pointing out this missing detail.

Action: In the methods section, we added the specification that the nutation experiments were recorded using rectangular pulses. Furthermore, the original Bruker files for the experiment are included in the dataset (file *acqus* in *NMR_data/Exp_nut_spectrum.rar*) that is to be published alongside the paper.

Revised Paragraph: Nutation experiments were performed with rectangular pulses of varying pulse length and a constant pulse power of 1.5 W. In total, 100 pulse lengths were screened ~~The pulse length list consisted of 100 points~~ with a step size of 30 µs.

4. Experiments with B0 field selectivity. They're generally clear, but my personal opinion is that before using special pulses, it would be worth demonstrating how standard selective pulses work for this phantom, such as a Gaussian or E-burb pulse, or others available in Topspin. Then it would be clearer to what extent special pulses are needed.

Response:

The results based on GRAPE-optimized QOC pulses were compared against E-BURP pulses on a freshly constructed model setup. The superior performance of the QOC approach is illustrated in a comparison of two waterfall spectra (analogously to Figure 3 and 4), detailing the application of QOC (a) versus E-BURP (b) pulses. Figure (a) shows again an efficient excitation within the selective bandwidth of the QOC pulse and a suppression of resonances outside of this bandwidth. While the E-BURP pulses in Figure (b) also manage to provide decently selective excitation of *n*-dodecane, the selective excitation of H_2O is imperfect and leads to higher residuals of *n*-dodecane signal compared to the use of QOC pulses. Additionally, the application of E-BURP pulses heavily distorts the baseline for some resonance frequency offsets and affects the shape of the *n*-dodecane peak when selectively exciting it. The most important individual spectra of the experiments (on-resonance pulses for *n*-dodecane and H_2O) were summarized in Figure S28 and added to the SI.

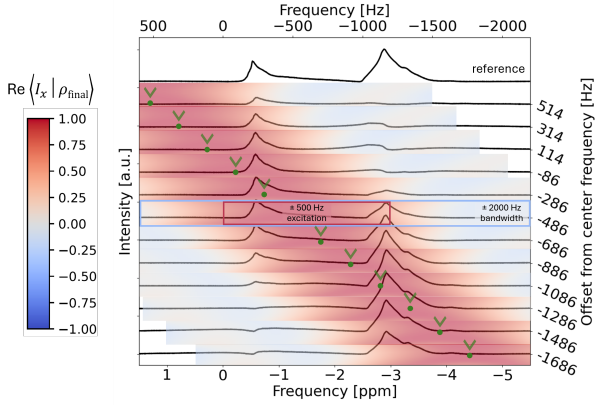

(a)

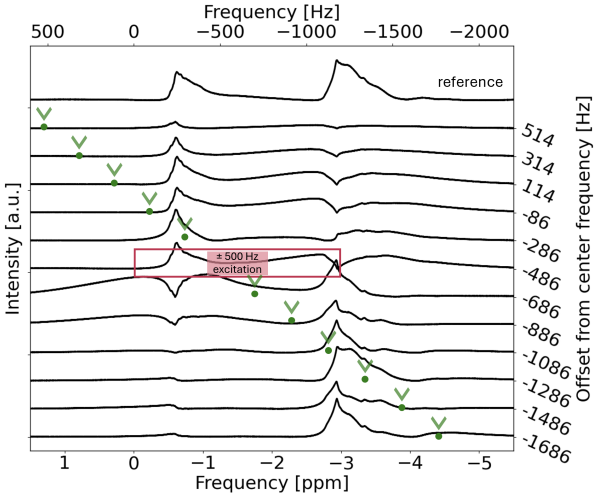

(b)

We assume that the poorer performance of E-BURP lies indeed in the lack of robustness against nutation frequency deviations, as strong residuals appear predominantly when attempting suppression of the signal associated with the Cu cavity. The BURP excitation pulses as originally published by Geen and Freeman (1991), therefore, seem to be only suited for Larmor-frequency selective measurements with unperturbed B_1, since suppression of the signal associated with the PEEK cavity was still satisfactory. In summary, the robustness against nutation frequency deviations enabled with QOC pulses provides a drastic improvement in selectivity for measurements in the vicinity of conductive surfaces.

Further reasons for using GRAPE over BURP regard pulse length. Pulses optimized in a Fourier basis tend to require longer pulse durations τ due to less flexibility in the pulse shape. For example, an excitation band of $\pm$500 Hz around the irradiation frequency, as used in our paper, corresponds to a BURP-1 pulse length of 4 ms according to the BURP-1 design rule $0 \leq \nu_{\mathrm{exc}} \leq 2/\tau$. Since GRAPE can optimize pulses with arbitrary shape within the piecewise-constant treatment, a shorter pulse duration of 1 ms was sufficient, while providing robustness against nutation frequency deviations on top. Shorter pulse durations are crucial for future applications in the electrochemical context. In particular, in operando applications and their temporal resolution depend critically on the duration of the individual pulse sequence as well as the selectivity and efficiency of the excitation (and suppression), as the latter one impacts how many repetitions have to be conducted to achieve a reasonable signal-to-noise. Furthermore, relaxation or dephasing may be enhanced in the vicinity of electrodes, which leads to broad lines. Having excitation pulses that are as short as possible to achieve a required selectivity is crucial to minimize the T_2 or $T_2^\star$ weighting effects. In addition, GRAPE-optimized pulses can have multiple excitation bands, which might find applications for CO_2 reduction producing various different solvated products in low concentrations, such as CO, methanol, ethanol, formic acid, etc.

Action:

Testing of E-BURP pulses and additions in conclusion as well as in the SI.

Revised Paragraph:

New figure:

Figure S28: ^{1}H spectra recorded utilizing a ν_0-selective QOC excitation pulse (1 ms) versus an E-BURP-1 pulse (4 ms) with a selective excitation range of 2.5 ppm ($\pm$500 Hz). The top spectrum depicts the reference ^{1}H spectrum recorded using a hard pulse. Hereby, the resonance at approx. -3.3 ppm is assigned to *n*-dodecane and the resonance at approx. -0.8 ppm to H_2O. The pulses were applied on-resonance for either H_2O (a) or *n*-dodecane (b). The selective excitation of *n*-dodecane is achieved to a similar degree with both pulses, while the selective excitation of water is less efficient when using the E-BURP-1 pulse. The E-BURP-1 pulse is observed to distort the spectrum baseline and excites the *n*-dodecane resonance to a significant degree. The shift in frequencies with respect to previous measurements (other figures) originates from a severe drift of the magnet in the

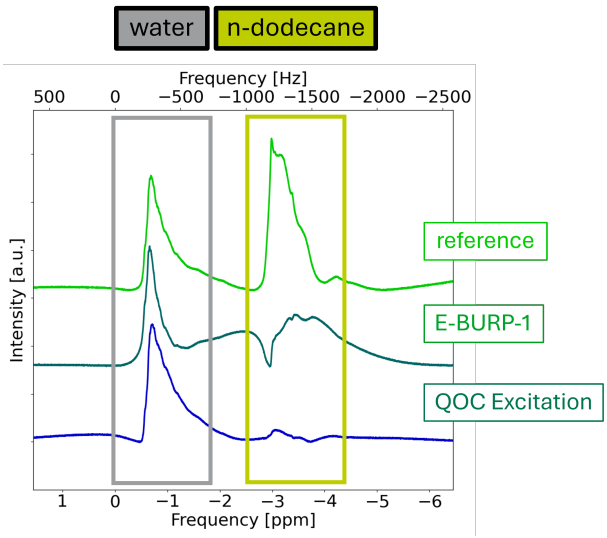

(a)

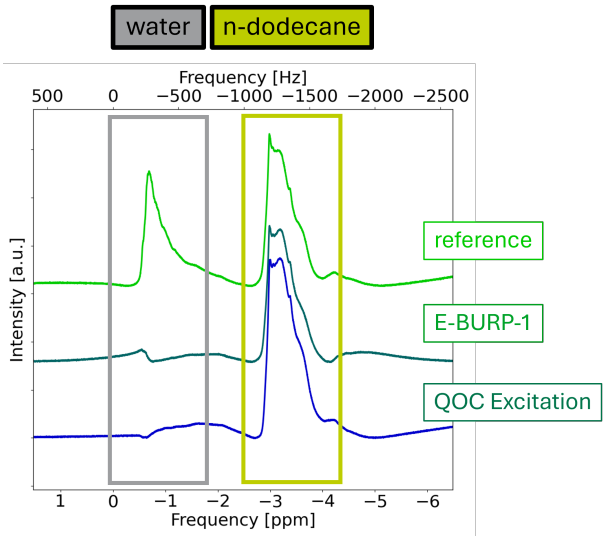

(b)

meantime.

Introduction

The rf modulation impedes the effectiveness of established selective pulse sequences such as BURP, which are not optimized for systems with inherently distorted B_1 fields Geen and Freeman (1991).

Conclusion

To support this claim, a comparison of QOC excitation pulses and E-BURP pulses on the herein presented model setup was undertaken (SI Fig. S28). The comparison evidently visualized, that when using literature-known ν_0-selective pulses without ν_1 robustness for electrochemical setups, baseline distortions and unsatisfactory selectivity may occur due to strong B_1 field distortions near conductive cell components. Furthermore, the B_1 field distortions ~~near conductive electrochemical cell components~~ in the model setup were accurately predicted by FEM and integrated into a QOC workflow to tailor pattern pulses which exploit the simulated sharp B_1 enhancement near conductive interfaces.

5. Figure 5 is about B1 selectivity. This graph is completely unclear. What is shown on the Y ordinate axis? How this graph or spectrum was obtained is unclear. The nutation frequency is shown in kHz at the top, and the B1 field in a.u. units at the bottom. I believe that if the nutation frequency for protons is known, then the B1 magnetic field magnitude can be expressed in microtesla.

Response:

Indeed, the dual x-axis structure can be disorienting and we thank the reviewer for pointing out this potential risk. We made adjustments to the figure and caption for better clarification. The unit of the bottom x-axis was changed to µT, leading to slight changes due to rounding (25.7% instead of 26.1%). Detailed information on how the nutation spectrum was measured was already given in the Methods section.

Action:

The plot was updated such that the x-axis of the FEM-simulation results are now given in µT. Furthermore, the caption now starts by emphasizing that Fig. 5 is a dual x-axis plot. It contains a brief description on how the nutation spectrum was recorded and how the FEM-histogram was obtained. We added a color-coded y-axis labels for more clarity. Scales on the y-axes were omitted as the absolute histogram counts and the absolute intensity are not relevant for the interpretation of the plot.

Revised Paragraph:

Results and Discussion

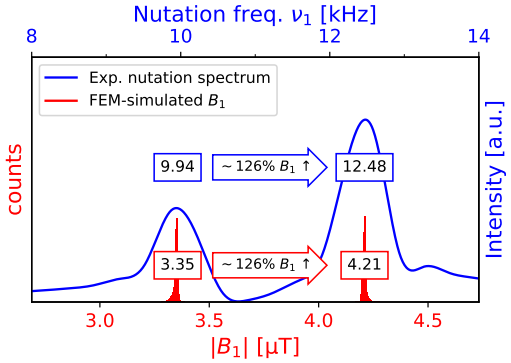

Figure 4 Dual x-axis plot superimposing the experimental ~~ν_1~~ nutation spectrum interpolated by a cubic spline (blue) ~~compared with~~ and the FEM-simulated B_1 distribution (red). The nutation spectrum was recorded using rectangular pulses of varying pulse length at a constant pulse power (see Sec. 2.2). The FEM-simulated B_1 distribution was obtained as a histogram of the B_1 magnitudes at all the finite volume elements of the cavities. The smaller ν_1 and B_1 correspond to the PEEK cavity while the bigger ν_1 and B_1 correspond to the copper cavity. The relative difference between the ν_1 maxima (~~25.5~~25.6 %) is in good alignment with the relative B_1 increase predicted by the FEM simulation (~~26.1 %~~25.7 %).

6. Figure C19 in the supplementary materials shows water on a gray background, although it's most likely represented by blue disks. It would be more accurate to indicate it with arrows or another method. At first glance, it appears that the entire gray area around it consists of water.

Response: We agree with the reviewer, that parts of the figure were ambiguous. The gray background was omitted and the positioning of the text adjusted.

Action: We revised the figure in question.

Revised Paragraph:

Experimental Setup (SI)

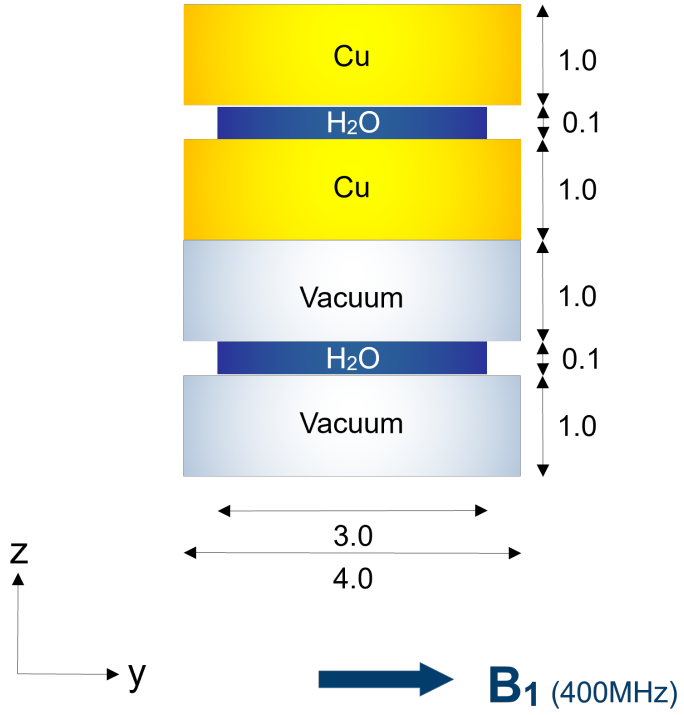

7. A general question regarding images c1-c4. It's clear that the amplitude of B1 over time has some high-frequency noise. How important is this noise? What determines the amplitude of this noise? What would happen if, instead of an amplitude pulse with high-frequency noise, we applied a pulse without this noise, but only with an envelope, after applying a low-pass filter?

Response:

The "noise" in the pulse shape is not noise. It is a byproduct of the numerical optimization process of GRAPE. GRAPE-pulses with complex tasks such as pattern pulses often exhibit unintuitive shapes (Kobzar et al., 2005). But this is not an annoyance. It is part of the solution determined by the GRAPE algorithm. Recently published phase-modulated ultrabroadband pulses also exhibit shapes resembling noise, but this "noise" is an integral part of the solution (see SI of (Woordes et al., 2026)). Thus, "smoothening" these pulse can potentially change the quantum dynamics and the pulse outcome. For example, applying a Butterworth low-pass filter to the nutation frequency selective pulses with a cutoff frequency of 50 kHz lead to a quality function decline of 1.1% in the case of $\Gamma_{B_1} = 1.25$. In the cases $\Gamma_{B_1} = 1.0$ and 1.8, the noise filter had negligible effect on the quality function. For the remaining pulses, the decline was between 0% and 1%. Although 1% does not feel like much, in ensemble optimal control, where many quality functions are averaged, a few percent can make a strong difference in pulse

performance. Luckily, modern spectrometers are well capable of faithfully implementing pulses with non-smooth shapes in a time resolution of sub-microseconds.

8. Line 51. The abbreviation PEM is not revealed.

Response:

We thank the reviewer for spotting this unassigned abbreviation, which escaped our proofreading .

Action:

We explained the abbreviation.

Revised Paragraph:

FEM simulations have also been utilized to validate and optimize uniform B_1 distribution within in operando cell setups to study proton exchange membrane (PEM) fuel cells (Zhang et al., 2011), as well as battery applications, (Aguilera et al., 2021; Sanders et al., 2022) up to commercial coin cell scales (Walder et al., 2021).

References

Aguilera, A. R., MacMillan, B., Krachkovskiy, S., Sanders, K. J., Alkhayri, F., Adam Dyker, C., Goward, G. R., and Balcom, B. J.: A parallel-plate RF probe and battery cartridge for ^{7}Li ion battery studies, J. Magn. Reson., 325, 106 943, https://doi.org/10.1016/j.jmr.2021.106943, 2021.

Geen, H. and Freeman, R.: Band-selective radiofrequency pulses, J. Magn. Reson., 93, 93–141, https://doi.org/https://doi.org/10.1016/0022-2364(91)90034-Q, 1991.

Kobzar, K., Luy, B., Khaneja, N., and Glaser, S. J.: Pattern pulses: design of arbitrary excitation profiles as a function of pulse amplitude and offset, J. Magn. Reson., 173, 229–235, https://doi.org/10.1016/j.jmr.2004.12.005, 2005.

Sanders, K. J., Aguilera, A. R., Keffer, J. R., Balcom, B. J., Halalay, I. C., and Goward, G. R.: Transient lithium metal plating on graphite: Operando ^{7}Li nuclear magnetic resonance investigation of a battery cell using a novel RF probe, Carbon, 189, 377–385, https://doi.org/10.1016/j.carbon.2021.12.082, 2022.

Schatz, M., Streun, M., Jovanovic, S., Eichel, R.-A., and Granwehr, J.: Workflow for systematic design of electrochemical in operando NMR cells by matching B_0 and B_1 field simulations with experiments, Magnetic Resonance, 5, 167–180, https://doi.org/10.5194/mr-5-167-2024, 2024.

Walder, B. J., Conradi, M. S., Borchardt, J. J., Merrill, L. C., Sorte, E. G., Deichmann, E. J., Anderson, T. M., Alam, T. M., and Harrison, K. L.: NMR spectroscopy of coin cell batteries with metal casings, Sci. Adv., 7, eabg8298, https://doi.org/10.1126/sciadv.abg8298, 2021.

Woordes, Y. T., Kobzar, K., Ehni, S., Görling, B., Schilling, F., Seliwjorstow, A., Pianowski, Z. L., Roesky, P. W., Bräse, S., Eppinger, J., Glaser, S. J., and Luy, B.: Ultrabroadband 1D and 2D NMR Spectroscopy, Angew Chem. Int. Ed., 65, e15 467, https://doi.org/https://doi.org/10.1002/anie.202515467, 2026.

Zhang, Z., Marble, A. E., MacGregor, R. P., Martin, J., Wang, H., and Balcom, B. J.: Zero-mode TEM parallel-plate resonator for high-resolution thin film magnetic resonance imaging, Can. J. Chem., 89, 745–753, https://doi.org/10.1139/v11-018, 2011.